Flexible and Wire-Shaped Micro-Supercapacitor Based on $Ni(OH)_2$-Nanowire and Ordered Mesoporous Carbon Electrodes

Xiaoli Dong, Ziyang Guo, Yanfang Song, Mengyan Hou, Jianqiang Wang, Yonggang Wang, and Yongyao Xia**

Portable and multifunctional electronic devices are developing in the trend of being small, flexible, roll-up, and even wearable, which asks us to develop flexible and micro-sized energy conversion/storage devices. Here, the high performance of a flexible, wire-shaped, and solid-state micro-supercapacitor, which is prepared by twisting a Ni(OH)2-nanowire fiber-electrode and an ordered mesoporous carbon fiber-electrode together with a polymer electrolyte, is demonstrated. This micro-supercapacitor displays a high specific capacitance of 6.67 mF cm^{-1} (or 35.67 mF cm^{-2}) and a high specific energy density of 0.01 mWh cm^{-2} (or 2.16 mWh cm^{-3}), which are about 10–100 times higher than previous reports. Furthermore, its capacitance retention is 70% over 10 000 cycles, indicating perfect cyclic ability. Two wire-shaped micro-supercapacitors (0.6 mm in diameter, ≈3 cm in length) in series can successfully operate a red light-emitting-diode, indicating promising practical application. Furthermore, synchrotron radiation X-ray computed microtomography technology is employed to investigate inner structure of the micro-device, confirming its solid-state characteristic. This micro-supercapacitor may bring new design opportunities of device configuration for energy-storage devices in the future wearable electronic area.

1. Introduction

The modern digital life has led us to an emerging ubiquitous information society, with an increasing need for multifunctional portable, roll-up and even wearable electronic devices as well as autonomous microsystems to develop wireless sensing and communication networks.[1–14] The design of these portable electronic devices with roll-up and wearable characters requires flexible energy storage devices as power sources (i.e., supercapacitors or Li-ion batteries).[1–14] Owing to the inherent characteristics of high power density, long cyclic life, and high efficiency, micro-supercapacitors are being considered as the most promising power sources for these portable and/or micrometer-sized electronic devices.[15–21] Unfortunately, technologies for developing sufficiently flexible micro-supercapacitors are still much more inadequate. Although flexible or/and micro-sized supercapacitors have been widely investigated, their structure generally keeps the basic two-dimensional (2-D) character or/and layer-by-layer construction of conventional supercapacitors that are potentially applied for bulky electronic devices.[3–6,8–10,12–21] Especially, a lot of micro-supercapacitors for on-chip energy storage, which are prepared by depositing or printing active materials on 2D solid state substrate,[16–19] still can not satisfy the demands from future flexible and wearable electronic devices.

Compared with the conventional 2-D planar structure, a wire-shaped and micrometer-sized energy storage device can be easily woven into textiles or other structures to exhibit unique and promising applications.[22,23] The limitation is originated from the much stricter requirement for the electrode such as a combined high flexibility and electrochemical property in wire-shaped devices. Only very recently, flexible and wire-shaped micro-supercapacitors were developed.[22–28] However, these wire-shaped micro-supercapacitors still display low capacitance (*F*) and energy (*Wh*) in area and length units. Therefore, it remains challenging but becomes highly desired to obtain wire-shaped micro-supercapacitors with high performances.

Herein, we have developed a flexible, wire-shaped and solid-state micro-supercapacitor with high electrochemical performance by twisting a $Ni(OH)_2$-nanowire fiber-electrode and an ordered mesoporous carbon fiber-electrode together with a gel state polymer electrolyte of poly (vinyl alcohol)-KOH (PVA-KOH). The wire-shaped micro-supercapacitor displays a maximum cell voltage of 1.5 V with a much high specific capacitance of 6.67 mF cm^{-1} (or 35.67 mF cm^{-2}) and a high specific energy density of 0.01 mWh cm^{-2} (or 2.16 mWh cm^{-3}). Furthermore, the capacitance retention of the wire-shaped

X. Dong, Z. Guo, Y. Song, M. Hou, Prof. Y. Wang, Prof. Y. Xia
Department of Chemistry and
Shanghai Key Laboratory of Molecular Catalysis and Innovative Materials
Institute of New Energy
Fudan University
Shanghai 200433, China
E-mail: ygwang@fudan.edu.cn; yyxia@fudan.edu.cn
Prof. J. Wang
Shanghai Institute of Applied Physics
Chinese Academy of Sciences
Shanghai 201204, P. R. China

DOI: 10.1002/adfm.201304001

micro-supercapacitor is 70% over 10 000 cycles, indicating good cyclic life.

2. Results and Discussion

2.1. Character and Performance of $Ni(OH)_2$-Nanowire Fiber-Electrode

In recent years, nanosized $Ni(OH)_2$ has attracted extensive attention as a promising electrode material for conventional pseudocapacitor, owing to its high capacitance arising from the fast Ni^{2+}/Ni^{3+} redox reaction.[29–32] However, it is still a new topic to build a flexible fiber-electrode based on nanosized $Ni(OH)_2$. Herein, the $Ni(OH)_2$ nanowires grown on a Ni-fiber were prepared by a facile hydrothermal method. It can be detected from **Figure 1**a that a Ni-fiber with the size of 100 μm in diameter is full coated by a $Ni(OH)_2$ layer to form a typical coaxial cable-like electrode. As shown in Figure 1b, the coaxial cable-like electrode exhibits a uniform out-diameter size of ≈300 μm. SEM images with higher magnifications indicate that the coating layer is made up of a lot of $Ni(OH)_2$ nanowires with a length of several microns which agglomerate together to form a network structure (Figure 1c,d). High resolution SEM image of the $Ni(OH)_2$ coating layer is shown in Figure 1e, where it can be clearly observed that the typical size of $Ni(OH)_2$ nanowires is 10 nm in diameter. TEM image shown in Figure 1f further confirms the nanowires morphology of the $Ni(OH)_2$ coating layer. X-ray diffraction (XRD) pattern indicates that the prepared sample is α-phase $Ni(OH)_2$ (Figure S1, Supporting Information). Transmission X-ray Microscopy (TXM) technology was employed to further characterize the as-prepared fiber-electrode, which also demonstrates the uniform $Ni(OH)_2$-nanowire/Ni-fiber coaxial cable-like structure (Figure 1g). Cyclic Voltammetry (CV) experiments carried out at various sweep rates in alkaline electrolyte (6 M KOH) were used to examine the redox processes occurring in the $Ni(OH)_2$-nanowire/Ni-fiber coaxial cable-like electrode [i.e., $Ni(OH)_2$-nanowire fiber-electrode], where a saturated calomel electrode (SCE) and a Pt-flake (1 cm × 1 cm) were used as reference and counter electrodes, respectively. As shown in **Figure 2**a, a couple of redox peaks is observed between 0.1 V and 0.35 V versus SCE (or between 0.35 V and 0.6 V vs NHE). These peaks correspond to the extraction and insertion of proton and can be represented by the following equation:[29–32]

$$Ni(OH)_2 + OH^- \leftrightarrow NiOOH + H_2O + e^- \quad (1)$$

These redox peaks still can be observed clearly even at the high scan rate of 10 000 mV s^{-1}, indicating the perfect rate performance. Figure 2b gives the charge-discharge curves of the $Ni(OH)_2$-nanowire fiber-electrode at different currents. The capacitance (C, F) of $Ni(OH)_2$-nanowire fiber-electrode was calculated by the following equation: $C = I \times t/\Delta V$, where I, t, and ΔV correspond to the discharge current, discharge time, and potential window for charge/discharge, respectively. The calculated capacitance was further converted into the length specific capacitance (C_L, mF cm^{-1}), the area specific capacitance (C_A, mF cm^{-2}) and the mass specific capacitance (C_m, F g^{-1}). As shown in Figure 2c, the $Ni(OH)_2$-nanowire fiber-electrode exhibits a length specific capacitance of 18 mF cm^{-1} and an area specific capacitance 195 mF cm^{-2} at the current of 0.5 mA. In view of the mass loading of $Ni(OH)_2$, the calculated mass specific capacitance is 270 F g^{-1} at the current of 0.5 mA (or current density of 7.5 A g^{-1} that is calculated based on the mass of $Ni(OH)_2$). Even at the high applied current of 2.5 mA, the C_L, C_A, and C_m of the $Ni(OH)_2$-nanowire fiber-electrode keep at 6.6 mF cm^{-2}, 70 mF cm^{-2} and 99 F g^{-1}, respectively. Herein, it also should be noted that the capacitance contribution from the

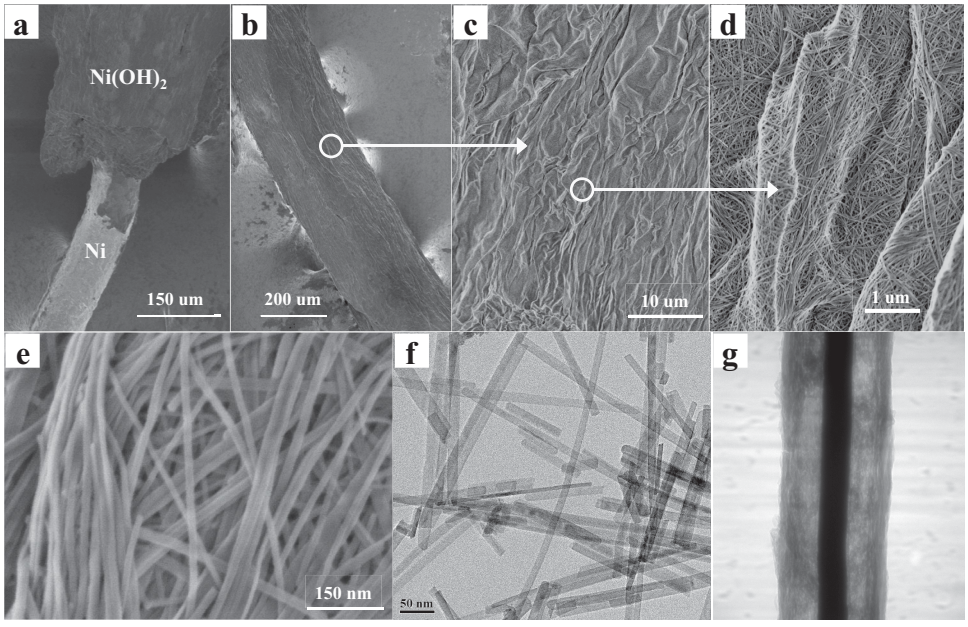

Figure 1. Microscopy measurements of $Ni(OH)_2$-nanowire fiber-electrode. a–e) SEM images with different magnifications. f) TEM image. g) TXM image.

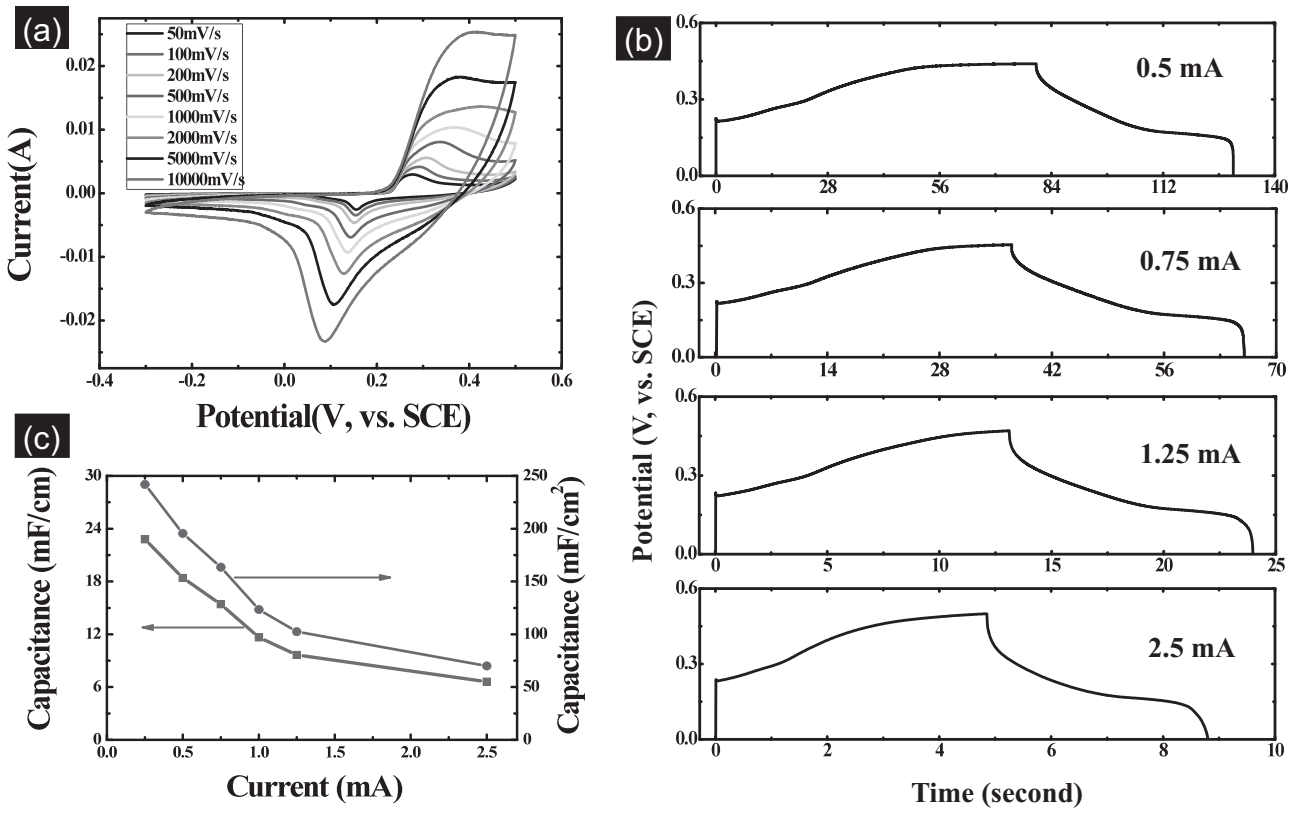

Figure 2. Electrochemical performance of $Ni(OH)_2$-nanowire fiber-electrode. a) CV curves within the potential window of –0.3–0.5 V (vs SCE) at different sweep rates. b) Charge/discharge curves with different currents. c) Length (or area) specific capacitance vs applied currents.

metallic Ni-fiber within the $Ni(OH)_2$-nanowire fiber-electrode can be neglected (see Figure S2, Supporting Information).

2.2. Character and Performance of Ordered Mesoporous Carbon Fiber-Electrode

Porous carbon materials with high surface area have been widely investigated as the electrode materials for electrochemical supercapacitors (i.e. electrochemical double layered capacitors, EDLCs), where the capacitance arises from the cations/anions adsorption on the surface of carbon electrode.[33] It has been well demonstrated that ordered mesoporous carbons (OMCs) with a narrow distribution in the mesopore range (2–5 nm) and a uniform pore connection have much better electrochemical performance than conventional porous carbon materials, due to that the mesopore channels and interconnections provide a more favorable path for penetration and transportation of ions.[34–36] However, up to present, the application of OMCs in micro-supercapacitor, especially the wire-shaped micro-supercapacitor, is rarely reported. Here, we prepared the OMC of FDU-15 according to previous report about FDU-15 synthesis,[37] and painted the as-prepared OMC on a Ni-fiber to form an OMC/Ni-fiber coaxial cable-like electrode [i.e., OMC fiber-electrode]. Detailed information about the preparation of the OMC fiber-electrode was given in the experimental section. TEM investigation demonstrates that the as-prepared OMC exhibits the typical ordered mesoporous structure which is consistent with previous report[37] (**Figure 3**). The small-angle X-ray scattering pattern (SAXS) of as-prepared OMC (i.e., FDU-15) is shown in Figure S3 (Supporting Information), revealing scattering peaks referring to (100), (110), and (200) reflections associated with 2D hexagonal p6m symmetry. N_2 sorption isotherm of as-prepared OMC shows representative type-IV curves with a H_2-type hysteresis loop, which is the typical character of mesoporous carbon (Figure S4a, Supporting Information). The pore size distribution (Figure S4b, Supporting Information) clearly demonstrates that the main pore size of the as-prepared OMC is 4.5 nm. The specific surface area of the as-prepared OMC is 675 $m^2 g^{-1}$, which is consistent with previous report.[37] The as-prepared OMC powders were dispersed into 5% nafion solution to form a slurry which was then painted on the Ni-fiber to form OMC/Ni-fiber coaxial cable-like electrode after drying. Electrochemical performance of the OMC/Ni-fiber coaxial cable-like electrode [i.e., OMC fiber-electrode] was investigated in 6 M KOH electrolyte solution with three-electrode system, where SCE and Pt-flake were used as reference and counter electrodes, respectively. CV curves of the OMC fiber-electrode at different scan rates are shown in **Figure 4**a, where rectangle CV curves can be observed clearly. In addition, CV profiles still retain a relatively rectangular shape without obvious distortion with increasing potential scan rates, even at a scan rate of 1000 mV s^{-1}, indicating the desirable fast charge/discharge property. It can be detected from Figure 4b that discharge/charge curves at different applied currents vary linearly with the test time, indicating a potential independent charge storage

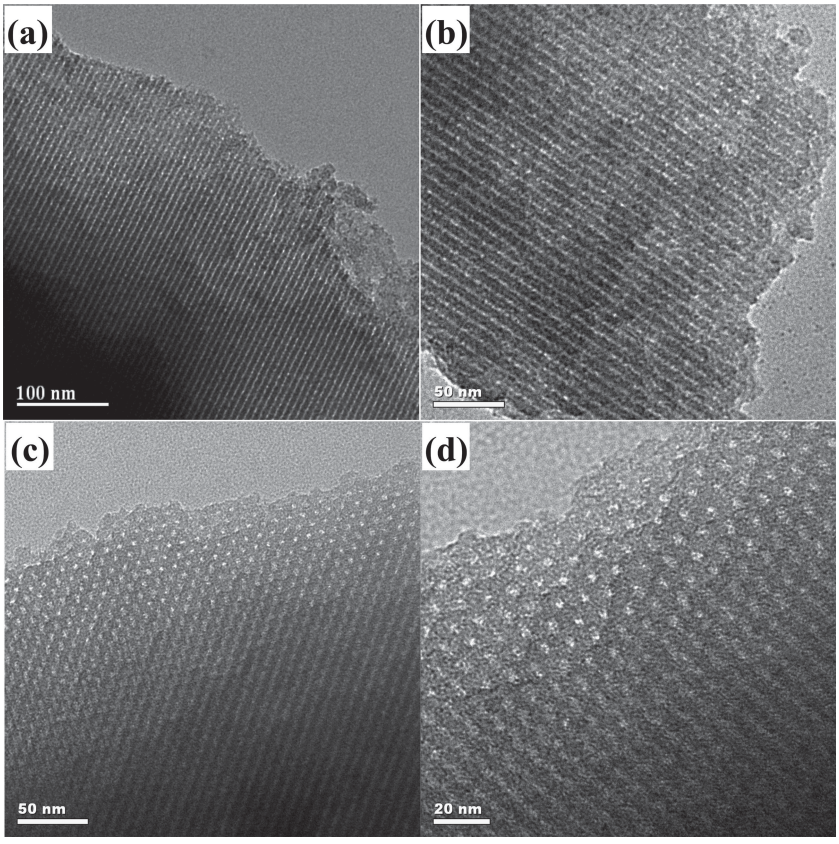

Figure 3. TEM images of as-prepared FDU-15 viewed at different directions.

characteristic of EDLCs.[33] The calculated specific capacitances of the OMC fiber-electrode according to discharge/charge investigation are summarized in Figure 4c. The OMC fiber-electrode delivers a C_L of 6.8 mF cm^{-1} and a C_A of 109 mF cm^{-2} at the current of 0.01 mA. According to the mass loading of OMC, the calculated mass specific capacitance of the OMC fiber-electrode is 76.7 F g^{-1} at current of 0.01 mA (or at the current density of 112 mA/g that is calculated based on the mass of OMC). At the current of 0.2 mA, the corresponding specific capacitances keep at 4 mF cm^{-1} and 64.5 mF cm^{-2}, respectively. Even at the high current of 2 mA, the OMC fiber-electrode still exhibits a C_L of 3 mF cm^{-1} and a C_A of 46 mF cm^{-2}, respectively.

2.3. Character and Performance of Wire-Shaped Micro-Supercapacitor

Next, we prepared a wire-shaped micro-supercapacitor by using the $Ni(OH)_2$-nanowire fiber-electrode and OMC fiber-electrode as positive electrode and negative electrode, respectively. In order to develop a practical wire-shaped micro-supercapacitor, gel state PVA-KOH solution was used as the solid electrolyte. Firstly, the $Ni(OH)_2$-nanowire fiber-electrode and OMC fiber-electrode were painted with PVA-KOH-H_2O solution. Then, the $Ni(OH)_2$-nanowire fiber-electrode and the OMC fiber-electrode were twisted together. Finally, a flexible and wire-shaped micro-supercapacitor was fabricated after further vaporizing water from the gel electrolyte (**Figure 5**a). The length and diameter of the wire-shaped micro-supercapacitor are about 3 cm and 0.6 mm, respectively (Inset of Figure 5a; Figure S5, Supporting Information). On charge process, proton is extracted from the framework of $Ni(OH)_2$ according to Equation 1 and cations (i.e., K^+ and H^+) in electrolyte simultaneously are absorbed in the pore structure of OMC.[29,32,38–42] Discharge reverses the charge process.[29,32,38–42] Figure 5b gives the charge/discharge curves of the wire-shaped micro-supercapacitor at different currents. As shown in Figure 5b, the wire-shaped micro-supercapacitor exhibits a maximum cell voltage of 1.5 V which arises from the potential difference between $Ni(OH)_2$ positive electrode (0–0.5 V vs SCE) and OMC negative electrode (–1 to 0 V vs SCE). This result is consistent with previous reports about conventional planar $Ni(OH)_2$/carbon supercapacitors.[29,32,38–42] The CV curve shown in Figure 5c of the wire-shaped micro-supercapacitor investigated at a scan rate of 500 mV s^{-1} indicates that its capacitance behavior mainly locates in the voltage window from 0.5 V to 1.5 V, which is consistent with the charge/discharge investigation. The specific capacitances of the wire-shaped micro-supercapacitor were calculated according to the charge/discharge investigations at different currents, and were summarized in Figure 5d. It can be detected that the wire-shaped micro-supercapacitor exhibits a C_L of 6.67 mF cm^{-1} and a C_A of 35.67 mF cm^{-2} at the current of 0.1 mA. The achieved specific capacitances are much higher than recent reports about wire-shaped supercapacitors[22–28] (detailed information about comparison is summarized in **Table 1**). In order to further compare with other systems, the mass specific capacitance of the wire-shaped micro-supercapacitor was also calculated based on the total mass of electrode active materials. The obtained value of 32 F g^{-1} achieved at the current of 0.1 mA was about 2–6× of other reports about wire-shaped micro-supercapacitors.[22,23] Even at the high current of 1 mA, the specific capacitances of the wire-shaped micro-supercapacitor still kept at 4 mF cm^{-1} in a length unit, 21.22 mF cm^{-2} in an area unit and 19.2 F g^{-1} in a mass unit, respectively (see Figure 5d). Besides the improved specific capacitances, the wire-shaped micro-supercapacitor developed in present work also displays higher cell voltage (1.5 V), compared with other reports about flexible supercapacitors with a maximum cell voltage that is less than 1 V.[22,24–28] The reason is that this wire-shaped micro-supercapacitor efficiently utilizes the different potential windows between the two kinds of electrodes (i.e., $Ni(OH)_2$ and the OMC) to increase the maximum cell voltage. It is well known that the energy density (E) of a supercapacitor depends on both the specific capacitance (C) and cell voltage (V), according to the equation $E = 1/2CV^2$.[33,36] Therefore, the energy density of present wire-shaped micro-supercapacitor is superior to previous

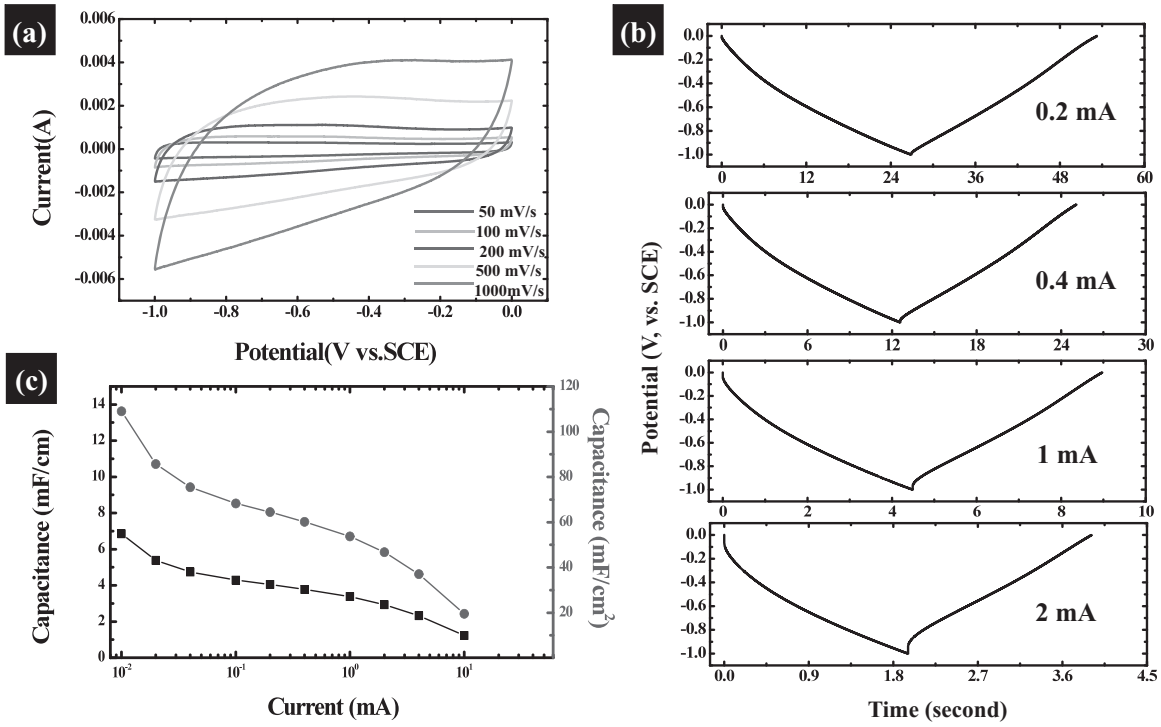

Figure 4. Electrochemical Performance of OMC fiber-electrode. a) CV curves within the potential window from 0 to –1 V (vs SCE) at different sweep rates. b) Charge/discharge curves with different currents. c) Length (or area) specific capacitance vs applied currents.

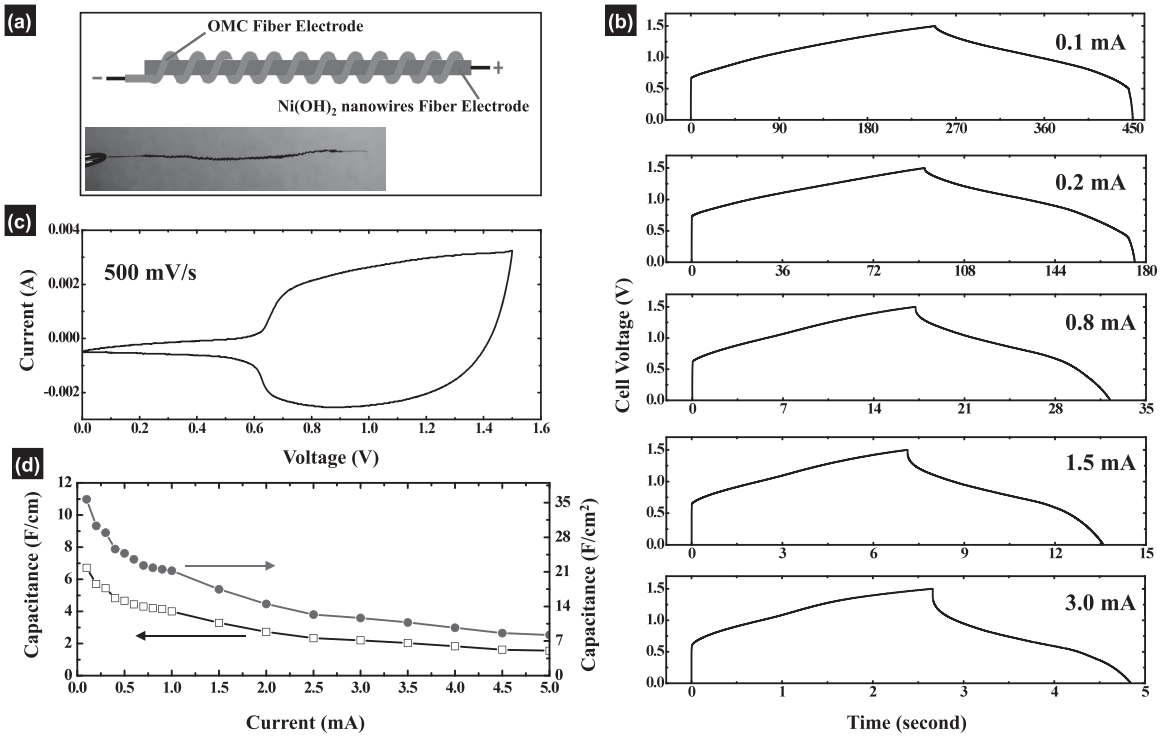

Figure 5. Fabrication and electrochemical performance of wire-shaped micro-supercapacitor. a) Schematic illustration of the micro-device (inset: photo of the device). b) Charge/discharge curves within the voltage window from 0 to 1.5 V at different currents. c) CV curve at the sweep rate of 500 mV s^{-1}. d) Length (or area) specific capacitance vs applied currents.

Table 1. Performance summary of recent reports about flexible and wire-shaped micro-supercapacitor.

C_L [mF cm^{-1}]	C_A [mF cm^{-2}]	E_A [mWh cm^{-2}]	E_V [mWh cm^{-3}]	P_A [mW cm^{-2}]	P_V [mW cm^{-3}]	Refs.
6.67	35.67	0.01	2.16	7.3	1600	Present Work
0.2	2.4	2.7×10^{-5}	/	1.4×10^{-2}	/	[22]
0.019	3.53	/	1.73	/	790	[23]
1.91	39.7	1.77×10^{-3}	/	4.3×10^{-2}	/	[24]
0.029	8.66	/	/	/	/	[25]
/	11.9–19.5	2.7×10^{-3}	/	0.042–9.1	/	[26]
0.018	1.2–1.7	1.7×10^{-4}	/	0.1	/	[27]
0.024	0.6	1.5×10^{-4}	/	/	/	[28]

"/ " means that these data were not given in the corresponding reference. C_L and C_A are the specific capacitance in length and area units. E_A and E_V are the specific energy in area and volume units. P_A and P_V are the specific power in area and volume units.

reports[22–28] (see Table 1 for detailed comparison), owing to its improved specific capacitance and enhanced cell voltage. The energy density for this wire-shaped micro-supercapacitor is calculated to be 0.01 mWh cm^{-2} and 2.16 mWh cm^{-3}, respectively, at the applied current of 0.1 mA [please see the ragone plot (power density vs energy density) in Figure S6, Supporting Information]. With the increase of current, this micro-device reaches its maximum average power density of 7.3 mW cm^{-2} and 1.6 W cm^{-3} at the applied current of 7 mA (Figure S6, Supporting Information). For comparison, we also prepared a wire-shaped symmetric micro-supercapacitor in which the same two OMC fiber-electrodes were used as positive electrode and negative electrode, respectively. The wire-shaped symmetric micro-supercapacitor only exhibits a maximum cell voltage of 1 V, and thus displays a lower energy density (see Figure S7 and corresponding discussion, Supporting Information), compared with the wire-shaped micro-supercapacitor based on $Ni(OH)_2$ and OMC electrodes. Cycling performance tested at an applied current of 0.5 mA of the wire-shaped micro-supercapacitor based on $Ni(OH)_2$ and OMC electrodes is shown in **Figure 6**a, where it can be observed that its capacitance retention is about 70% over 10 000 cycles, indicating good cyclic life. Figure 6b gives the charge/discharge curves of the wire-shaped micro-supercapacitor at different bending states with a test current of 0.4 mA. As shown in Figure 6b, the charge/discharge performance of the wire-shaped micro-supercapacitor is almost independent of the bending states, indicating its flexible characteristic. Furthermore, electrochemical impedance spectroscopy (EIS) investigation of the wire-shaped micro-supercapacitor also demonstrates that the internal resistance of the micro-supercapacitor almost keeps at a constant value at different bending states, further confirming its flexible characteristic (please see Figure S8 for details, Supporting Information). After being charged to 3 V for about 80 s, two wire-shaped micro-supercapacitors (0.6 mm in diameter and ≈3 cm in length for each unit) in series can successfully operate a red LED light (the lowest working voltage is 1.5 V)

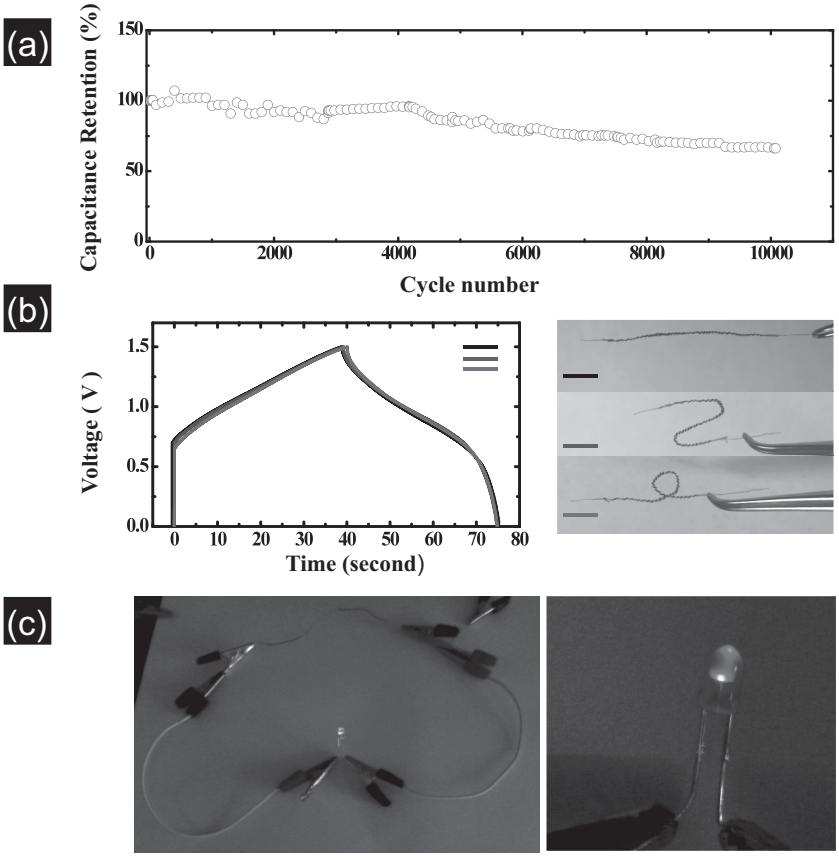

Figure 6. Stability and demo application of wire-shaped micro-supercapacitor. a) Cyclic performance (investigated at an applied current of 0.5 mA within the voltage window from 0 V to 1.5 V). b) Charge/discharge curves at different bending states. c) Digital photo that shows two micro-devices in series to light a LED.

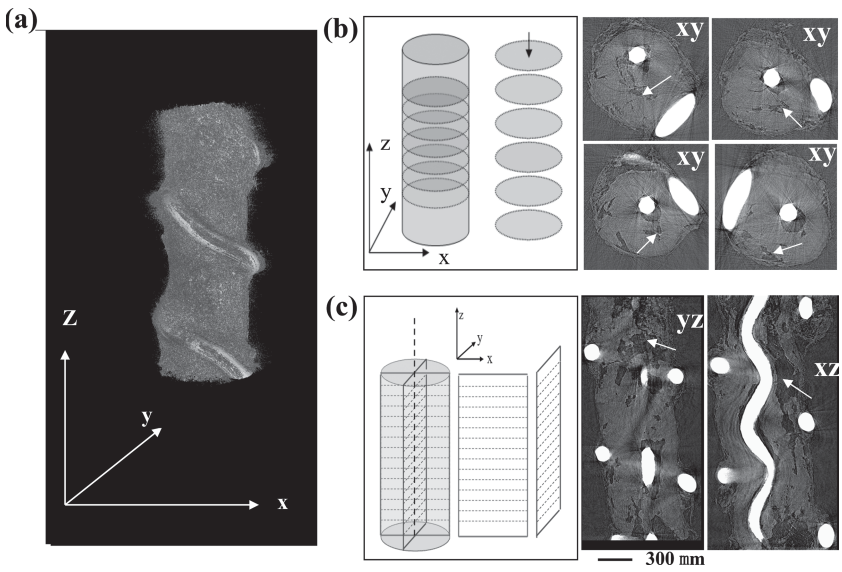

Figure 7. SR-μCT investigation of wire-shaped micro-supercapacitor. a) Reconstructed 3D image. b) Reconstructed images of 2D slices at *x*–*y* plane with different *z* values. c) Reconstructed images of 2D slices at *y*–*z* plane and *x*–*z* plane.

for about 40 s (Figure 6c). [After being charged to 4 V for 60 s, three wire-shaped micro-supercapacitors (≈2 cm in length for each unit) can light a LED with lowest working voltage of 2.0 V for 30 s. See Figure S9, Supporting Information.] Although the supercapacitor-powered LEDs have been widely demonstrated in previous investigations,[3,6,8–10,14,19,21] such small-sized micro-supercapacitors (especially for these flexible and wire-shaped micro-supercapacitors[22–28] are rarely reported for powering LED. This result further demonstrates the high performance of the wire-shaped micro-supercapacitor, and indicates its potential practical application.

Finally, synchrotron radiation X-ray computed microtomography (SR-μCT) technology was employed to investigate the inner structure of the wire-shaped micro-supercapacitor. As shown in **Figure 7**a, the reconstructed three dimensional (3D) image of the wire-shaped micro-supercapacitor exhibits a typical twisting structure which is consistent with the schematic illustration and photo of the micro-supercapacitor shown in Figure 5a. Figure 7b gives the reconstructed images of 2D slices at *x*–*y* plane with different *z* values, where it can be clearly detected that the solid-state electrolyte is well dispersed around the fiber-electrodes, further confirming the all-solid-state characteristic of the micro-supercapacitor. However, some defects can also be observed in the 2D slices at *x*–*y* plane (see arrows in these images). In order to further clarify this point, we also reconstructed the images of 2D slices at *y*–*z* plane and *x*–*z* plane which demonstrates the existence of defects within the solid-state micro-supercapacitor (Figure 7c). These observed defects should be attributed to that some porous structures within these coaxial cable-like electrodes (i.e., $Ni(OH)_2$-nanowire fiber-electrode and OMC fiber-electrode) are not filled with the solid-state electrolyte. This phenomenon may limit the ions diffusion at high rate charge/discharge of the devices, which should be improved in our future investigation. However, solid-state electrolyte distribution in a micro-sized device is still a great challenge, which needs not only new electrolyte materials but also advanced analysis technology for observing the inner structure of micro-sized devices. Although the SR-CT technology at nano- and microscale is attracting extensive attention from various research fields,[43] its application in flexible and micro-sized energy storage/conversion devices is still a new topic. It is expected that the primary results mentioned above can provide a paradigm for SR-CT application in the investigation of flexible and micro-sized energy storage/conversion devices.

3. Conclusion

Summarily, a flexible, wire-shaped and solid-state micro-supercapacitor with a maximum cell voltage of 1.5 V has been successfully designed and prepared by twisting a $Ni(OH)_2$-nanowire fiber-electrode and an ordered mesoporous carbon fiber-electrode together. The unique nanostructure of active materials and the coaxial cable-like electrode architecture offer a remarkable electrochemical performance including high specific capacitance and cyclic stability. The flexible wire-shaped structure enables the promising applications in various flexible electronic devices. This work also presents a fabrication paradigm in the development of high performance flexible and micro-sized energy storage devices by optimizing nanostructure of electrodes and choosing proper electrodes couple.

4. Experimental Section

Synthesis of $Ni(OH)_2$-Nanowire/Ni-Fiber Coaxial Cable-like Electrode: in the typical preparation of $Ni(OH)_2$ nanowires, 10 mL aqueous solution including 9.8 mmol NaOH was slowly added into a 30 mL aqueous solution containing 9.8 mmol $NiSO_4{\cdot}6H_2O$ under stirring condition. Afterwards, the reaction solution was transferred into a 50 mL capacity Teflon-lined stainless steel autoclave where several Ni fibers (0.1 mm in diameter) have already been put into. The autoclave was then sealed and maintained at 120 °C for 24 h in the electric oven. After hydrothermal treatment, $Ni(OH)_2$ nanowires were grown on Ni wires. Taken out carefully, washed with deionized water for several times and then dried in air at 80 °C for 12 h, Ni-supported $Ni(OH)_2$ nanowires were finally obtained. In the $Ni(OH)_2$-nanowire/Ni-fiber coaxial cable-like electrode [i.e., $Ni(OH)_2$-nanowire fiber-electrode], the mass loading of $Ni(OH)_2$ is about 0.2 mg/3 cm.

Preparation of OMC/Ni-Fiber Coaxial Cable-like Electrode: the synthesis of ordered mesoporous carbon FDU-15 is according to the reported procedure,[37] and the detailed information about preparation process is given in the supporting information section. The as-prepared OMC powders (85 wt%) were mixed with acetylene black (15 wt%), and then was dispersed into a nafion solution (5%) to form a slurry which was then painted on Ni fiber (0.1 mm in diameter) to form an OMC/Ni-fiber coaxial cable-like electrode after drying. In the OMC/Ni-fiber coaxial cable-like electrode [i.e., OMC fiber-electrode], the mass loading of OMC is about 0.2 mg/3 cm.

Preparation of Wire-Shaped Micro-Supercapacitor: Firstly, the $Ni(OH)_2$-nanowire fiber-electrode and OMC fiber-electrode were painted with PVA-KOH-H_2O solution. (Preparation of the PVA-KOH-H_2O solution is

given in Supporting Information.) Then, the $Ni(OH)_2$-nanowire fiber-electrode (about 3 cm in length) and the OMC fiber-electrode (about 6 cm in length) were twisted together. Finally, a flexible and wire-shaped micro-supercapacitor was fabricated after further vaporizing water from the gel electrolyte. The length and diameter of the wire-shaped micro-supercapacitor are about 3 cm and 0.6 mm, respectively. The total masses of $Ni(OH)_2$ and OMC (i.e., FDU-15) in the micro-supercapacitor are about 0.2 mg and 0.4 mg, respectively.

Electrochemical Investigation: The electrochemical performance of $Ni(OH)_2$-nanowire fiber-electrode and OMC fiber-electrode in alkaline electrolyte (6 M KOH) were investigated by three-electrode system where a saturated calomel electrode (SCE) and a Pt-flake (1 cm × 1 cm) were used as reference and counter electrodes, respectively. The as-prepared wire-shaped micro-supercapacitor was investigated as a two-electrode device where $Ni(OH)_2$-nanowire fiber-electrode and OMC fiber-electrode were used as positive electrode and negative electrode, respectively. Electrochemical work-station (CHI 660D) was employed for galvanostatic charge/discharge and cyclic voltammetry measurements. Detailed information about the calculations of specific capacitance, energy density and power density is given in the supporting information section.

Characterization of the Materials: XRD data for the prepared $Ni(OH)_2$ crystal was acquired with a Bruker D4 Endeavor X-ray diffractometer using Cu-Ka radiation. SEM images were recorded on a field emission SEM (FE-SEM s-4800). TEM experiments were conducted on a JEOL 2011 microscope (Japan) operated at 200 kV. SR-μCT tomographic images were acquired with beamline BL13W1 at Shanghai Synchrotron Radiation Facility (SSRF). Detailed information about the SR-μCT measurement and the characterization about FDU-15 are given in the supporting information section.

Acknowledgements

The authors acknowledge funding support from the Natural Science Foundation of China (21373060, 21333002), the State Key Basic Research Program of PRC (2013CB934103), Shanghai Pujiang Program (13PJ1400800) and Shanghai Science & Technology Committee (11DZ1100207, 08DZ2270500).

Received: November 27, 2013
Revised: December 29, 2013
Published online: February 13, 2014

[1] H. Nishide, K. Oyaizu, *Science* **2008**, *319*, 737.
[2] L. B. Hu, H. Wu, F. L. Mantia, Y. Yang, Y. Cui, *ACS Nano* **2010**, *4*, 5843.
[3] C. Z. Meng, C. H. Liu, L. Z. Chen, C. H. Hu, S. S. Fan, *Nano Lett.* **2010**, *10*, 4025.
[4] L. B. Hu, W. Chen, X. Xie, N. Liu, Y. Yang, H. Wu, Y. Yao, M. Pasta, H. N. Alshareef, Y. Cui, *ACS Nano* **2011**, *5*, 8904.
[5] X. Xu, X. Peng, H. Y. Jin, T. Q. Li, C. C. Zhang, B. Gao, B. Hu, K. F. Huo, J. Zhou, *Adv. Mater.* **2013**, *25*, 5091.
[6] A. Sumboja, C. Y. Foo, X. Wang, P. S. Lee, *Adv. Mater.* **2013**, *25*, 2809.
[7] K. H. Choi, S. J. Cho, S. H. Kim, Y. H. Kwon, J. Y. Kim, S. Y. Lee, *Adv. Funct. Mater.* **2014**, *24*, 44.
[8] Z. Q. Niu, H. B. Dong, B. W. Zhu, J. Z. Li, H. H. Hng, W. Y. Zhou, X. D. Chen, S. S. Xie, *Adv. Mater.* **2013**, *25*, 1058.
[9] L. Y. Yuan, X. H. Lu, X. Xiao, T. Zhai, J. J. Dai, F. C. Zhang, B. Hu, X. Wang, L. Gong, J. Chen, C. G. Hu, Y. X. Tong, J. Zhou, Z. L. Wang, *ACS Nano* **2012**, *6*, 656.
[10] Y. X. Xu, Z. Y. Lin, X. Q. Huang, Y. Liu, Y. Huang, X. F. Duan, *ACS Nano* **2013**, *7*, 4042.
[11] Y. H. Kwon, S. W. Woo, H. R. Jung, H. K. Yu, K. Kim, B. H. Oh, S. Ahn, S. Y. Lee, S. W. Song, J. Cho, H. C. Shin, J. Y. Kim, *Adv. Mater.* **2012**, *24*, 5192.
[12] M. Q. Xue, Z. Xie, L. S. Zhang, X. L. Ma, X. L. Wu, Y. G. Guo, W. G. Song, Z. B. Li, T. B. Cao, *Nanoscale* **2011**, *3*, 2703.
[13] J. Duay, E. Gillette, R. Liu, S. B. Lee, *Phys. Chem. Chem. Phys.* **2012**, *14*, 3329.
[14] X. H. Lu, M. H. Yu, T. Zhai, G. M. Wang, S. L. Xie, T. Y. Liu, C. L. Liang, Y. X. Tong, Y. Li, *Nano Lett.* **2013**, *13*, 2628.
[15] W. Gao, N. Singh, L. Song, Z. Liu, A. L. M. Reddy, L. J. Ci, R. Vajtai, Q. Zhang, B. Q. Wei, P. M. Ajayan, *Nature Nanotech.* **2011**, *6*, 496.
[16] J. Chmiola, C. Largeot, P. L. Taberna, P. Simon, Y. Gogotsi, *Science* **2010**, *328*, 480.
[17] D. Pech, M. Brunet, H. Durou, P. H. Huang, V. Mochalin, Y. Gogotsi, P. L. Taberna, P. Simon, *Nature Nanotech* **2010**, *5*, 651.
[18] D. Pech, M. Brunet, P. L. Taberna, P. Simon, N. Fabre, F. Mesnilgrente, V. Conedera, H. Durou, *J. Power Sources* **2010**, *195*, 1266.
[19] M. F. El-Kady, R. B. Kaner, *Nat. Commun.* **2013**, *4*, 1475.
[20] J. W. Long, B. Dunn, D. R. Rolison, H. S. White, *Chem. Rev.* **2004**, *104*, 4463.
[21] D. Kim, G. Shin, Y. J. Kang, W. Kim, J. S. Ha, *ACS Nano* **2013**, *7*, 7975.
[22] J. Bae, M. K. Song, Y. J. Park, J. M. Kim, M. L. Liu, Z. L. Wang, *Angew. Chem. Int. Ed.* **2011**, *50*, 1683.
[23] J. Ren, L. Li, C. Chen, X. L. Chen, Z. B. Cai, L. B. Qiu, Y. G. Wang, X. R. Zhu, H. S. Peng, *Adv. Mater.* **2013**, *25*, 1155.
[24] J. Ren, W. Y. Bai, G. Z. Guan, Y. Zhang, H. S. Peng, *Adv. Mater.* **2013**, *25*, 5965.
[25] X. L. Chen, L. B. Qiu, J. Ren, G. Z. Guan, H. J. Lin, Z. T. Zhang, P. N. Chen, Y. G. Wang, H. S. Peng, *Adv. Mater.* **2013**, *25*, 6436.
[26] Y. P. Fu, X. Cai, H. W. Wu, Z. B. Lv, S. C. Hou, M. Peng, X. Yu, D. C. Zou, *Adv. Mater.* **2012**, *24*, 5713.
[27] Y. N. Meng, Y. Zhao, C. G. Hu, H. H. Cheng, Y. Hu, Z. P. Zhang, G. Q. Shi, L. T. Qu, *Adv. Mater.* **2013**, *25*, 2326.
[28] T. Chen, L. B. Qiu, Z. B, Yang, Z. B. Cai, J. Ren, H. P. Li, H. J. Lin, X. M. Sun, H. S. Peng, *Angew. Chem. Int. Ed.* **2012**, *51*, 11977.
[29] H. B. Li, M. H. Yu, F. X. Wang, P. Liu, Y. Liang, J. Xiao, C. X. Wang, Y. X. Tong, G. W. Yang, *Nat. Commun.* **2013**, *4*, 1894.
[30] H. L. Wang, H. S. Casalongue, Y. Y. Liang, H. J. Dai, *J. Am. Chem. Soc.* **2010**, *132*, 7472.
[31] G. W. Yang, C. L. Xu, H. L. Li, *Chem. Commun.* **2008**, 6537.
[32] Y. G. Wang, Y. Y. Xia, *J. Electrochem. Soc.* **2006**, *153*, A743.
[33] P. Simon, Y. Gogotsi, *Nat. Mater.* **2008**, *7*, 845.
[34] H. J. Liu, J. Wang, C. X. Wang, Y. Y. Xia, *Adv. Energy Mater.* **2011**, *1*, 1101.
[35] H. Q. Li, R. L. Liu, D. Y. Zhao, Y. Y. Xia, *Carbon* **2007**, *45*, 2628.
[36] Y. G. Wang, Y. Y. Xia, *Adv. Mater.* **2013**, *25*, 5336.
[37] Y. Meng, D. Gu, F. Q. Zhang, Y. F. Shi, H. F. Yang, Z. Li, C. Z. Yu, B, Tu, D. Y. Zhao, *Angew. Chem. Int. Ed.* **2005**, *44*, 7053.
[38] J. Yan, Z. J. Fan, W. Sun, G. Q. Ning, T. Wei, Q. Zhang, R. F. Zhang, L. J. Zhi, F. Wei, *Adv. Funct. Mater.* **2012**, *22*, 2632.
[39] C. C. Hu, J. C. Chen, K. H. Chang, *J. Power Sources* **2013**, *221*, 128.
[40] J. W. Lang, L. B. Kong, M. Liu, Y. C. Lou, L. Kang, *J. Solid State Electrochem.* **2010**, *14*, 1533.
[41] Y. G. Wang, D. D. Zhou, D. Zhao, M. Y. Hou, C. X. Wang, Y. Y. Xia, *J. Electrochem. Soc.* **2013**, *160*, A98.
[42] Z. Tang, C. H. Tang, H. Gong, *Adv. Funct. Mater.* **2012**, *22*, 1272.
[43] A. Sakdinawat, D. Attwood, *Nat. Photonics* **2010**, *4*, 840.